

Heat transfer characteristics of an array of protruding elements in single phase forced convection

S. V. GARIMELLA and P. A. EIBECK

Department of Mechanical Engineering, University of California at Berkeley, Berkeley, CA 94720, U.S.A.

(Received 27 June 1989 and in final form 1 February 1990)

Abstract—Experiments are performed to determine the convective heat transfer coefficients for water cooling of inline and staggered arrays of 30 heated protruding elements arranged in six rows. The channel-height-based Reynolds number ranges from 150 to 5150. The channel height is varied over values of 1.2, 1.9, 2.7, and 3.6 element heights. The streamwise and spanwise spacings between elements are varied over a maximum of five values in the range of 0.5–6.5 element heights at each channel height. Pressure drops are measured in all cases. Transition Reynolds numbers are deduced from the heat transfer data. The data for all spacings are correlated using an array Reynolds number which accounts for a partitioning of the flow into bypass and array flows. Prandtl-number scaling of the results between air and water is investigated.

INTRODUCTION

THE RAPID advances in the computer industry have resulted in an increased need for reliable and efficient cooling technologies. Present trends in micro-electronics indicate that gate density will continue to increase as integrated circuits achieve higher speeds. Since almost all of the electrical energy consumed by these devices appears as heat, the power density that must be dissipated by individual chips will rise at a rapid rate. At the same time, overall systems packaging is being made as compact as possible, resulting in increased power densities at the module (group of chips) level and at the circuit board level.

The primary methods available for the cooling of electronic equipment include free and forced convection using air or liquid as the coolant. Air cooling has been the most popular method due to the simplicity it affords in cooling design. However, limitations in the cooling ability of air have necessitated the use of liquid coolants in modern mainframe computers. For indirect liquid cooling, water can be used because of its excellent thermophysical properties. Liquids with much higher dielectric strengths such as fluorocarbons are required if the coolant comes in direct contact with the electronics. The coolant could undergo a phase change to take advantage of the associated high heat transfer rates. However, boiling introduces problems such as acoustic and electrical noise, cavitation, and boiling hysteresis.

Single phase liquid cooling provides the most attractive alternative for high-heat-flux applications when the effectiveness of air cooling reaches its limits. High cooling rates can be achieved by single phase liquid cooling while avoiding the reliability and noise problems of two phase cooling. In spite of the large

number of studies dealing with electronics cooling in the literature, investigations of single phase liquid cooling of arrays of inline and staggered heated protruding elements appear to be unavailable [1].

A number of fundamental questions pertaining to the forced convection cooling of electronic components, especially in the context of liquid cooling, can be identified. In spite of several recent efforts, an adequate understanding of these issues is lacking. Questions include: (1) Under what conditions does a laminar-to-turbulent transition occur in channels containing large protruding elements? (2) Do heat transfer characteristics scale on Prandtl number from air to liquids? (3) What is the contribution of buoyancy to the total heat transfer in a forced convection situation? (4) What are the appropriate characteristic dimensions to be used in non-dimensionalization? (5) What is the extent of heat transfer enhancement obtained by staggering the elements of an array relative to an inline arrangement?

An extensive experimental study was undertaken to investigate the problems identified above. The objectives of the study were: (1) to provide generalized single-phase liquid cooling correlations useful to the electronics packaging designer and (2) to gain physical insight into the role of large protruding elements in influencing mixing and hence, heat transfer. Experiments were conducted on an array of heated protruding elements in a horizontal water channel. The dimensions of the simulated chips were held constant while the height of the channel and the streamwise and spanwise spacings between elements were varied. Heat transfer coefficients were obtained over a range of flow rates spanning the laminar and turbulent regimes. Pressure drop across the array was measured during all the experiments.

elements was installed in the bottom wall of the test section, and the temperature of each element was measured over a range of flow rates and heat fluxes. Four different channel heights were used and the streamwise as well as the spanwise spacings between elements were varied over a maximum of six values each. Flow visualization was carried out using dye entrainment and hydrogen bubbles. Details of the experimental setup and methods are presented below.

The water channel

The experiments were performed in a water channel with a 36.6 cm by 6.7 cm cross section and a total length of 180.3 cm. A schematic of the flow loop is shown in Fig. 1. The overhead reservoir provides a constant head for the gravity-fed water supply into the flow channel. Water enters the horizontal channel through a 5 cm i.d. pipe and is smoothly expanded to the full channel cross section in a diverging section that has side walls machined to a fifth-order polynomial shape designed to minimize separation. A combination of five screens and a 7.6 cm length of honeycomb are located upstream of the test section to produce a uniform flow across the channel cross section. All walls of the channel were fabricated from 1.9 cm thick Plexiglas.

The aspect ratio of the test section can be varied using a splitter plate that can be positioned at four different vertical locations of 1.4, 2.2, 3.2 and 4.2 cm from the bottom surface. As shown in Fig. 1, the splitter plate extends from 9 cm downstream of the screens to the end of the channel. Water exits from the two channels through separate pipes and is collected in the overflow tank, to be pumped back into the overhead reservoir. The lower of the two channels has two screens in the exit section to prevent propagation of exit disturbances upstream. One valve at the inlet and two downstream are used to set the required flow rates in the two channels formed by the splitter plate. A rotameter is installed in each of the two exit lines to measure flow rate. To improve the accuracy of reading, three rotameters with ranges of 0–10, 2–20, and 5–50 gallons per minute (0–631, 126–1262, and 315–3155 $\text{cm}^3 \text{s}^{-1}$) are used as necessary at the exit of the lower channel.

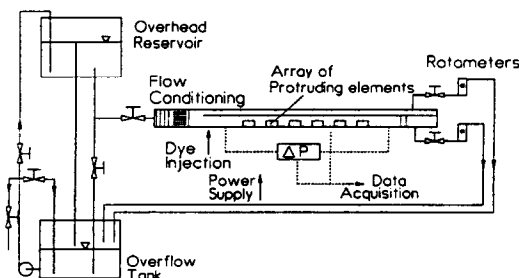


FIG. 1. Schematic of the liquid cooling test facility.

Test section

A detailed view of the test section is provided in Fig. 2(a). Flow rates in the two channels are adjusted so that the flow approaching the leading edge of the splitter plate passed smoothly over, without causing a separation bubble on either side. The leading edge of the plate has a bullet-shaped profile. Hydrogen bubbles and dye sheets were used to establish the uniformity of flow passing over the splitter plate as well as downstream of the leading edge. In what follows, the term water channel will be used to denote the lower of the two flow paths formed by the splitter plate.

The bottom wall of the channel is equipped with two detachable hatches fabricated from 2.5 cm thick Plexiglas. The smaller upstream hatch is 31.5 cm wide and 10.2 cm long and houses dye wells with slits spanning the width of the channel. The slits are located 14 and 23 cm upstream of the first row of heat source elements. Uniform sheets of dye can be entrained in the flow from either slit for flow visualization. This hatch can be replaced by another hatch which holds a 25 μm nichrome wire strung spanwise to generate hydrogen bubbles in the flow. This wire is held taut between two supports projecting into the flow from the hatch. The support rods can be moved up and down through compression fittings in the hatch so that hydrogen-bubble tracers are produced at any height in the channel.

The larger hatch is 31.5 cm wide and 45.7 cm long and constitutes the bottom wall of the test section. Thirty heated elements are mounted on this hatch in six spanwise rows of five elements each. Details of the heat source assembly are provided in Fig. 2(b). Each element consists of a copper block (2.54 cm by 2.54

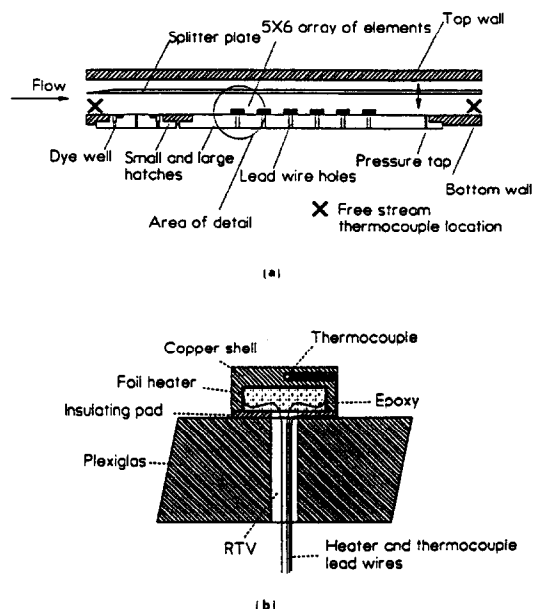


FIG. 2. (a) Schematic of the test section. (b) Detail of the heat source assembly.

cm by 1 cm high) that is partially hollowed out from the bottom face. A square, 100 W thin-film heater, 1.9 cm on the side, is attached with thermally conducting epoxy (Epo-Tek 930-1, $k = 2.2 \text{ W m}^{-1} \text{ K}^{-1}$) to the underside of the top face. This epoxy is made from boron nitride and is electrically insulating. The hollow is filled with the same epoxy. A thin square of high-density polyethylene (0.16 cm thick) is used to provide an insulating base ($k = 0.4 \text{ W m}^{-1} \text{ K}^{-1}$). The entire assembly was clamped and cured in a furnace. One thermocouple is located in a 0.2 cm diameter hole drilled from the back, halfway into the top face of the block as shown in Fig. 2(b). The hole is filled with epoxy to provide adhesion and thermal contact for the thermocouple junction. The elements are mounted on the hatch at prescribed spacings and the heater and thermocouple lead wires extend through 0.6 cm diameter holes drilled in the hatch under each element.

The heaters have a nominal resistance of 7Ω each and are designed for 25 V operation. The heaters are made from Inconel etched foil, sandwiched between Kapton insulating sheets. All heaters are connected in parallel across a pair of bus bars and operated at the same voltage. Inconel was chosen as the heating foil material due to its negligible temperature coefficient of resistance ($0.0001 \Omega \Omega^{-1} \text{ K}^{-1}$). Voltage and resistance were measured using a Fluke Digital Multimeter (model 8520A), with an accuracy of 0.004 V and 0.001Ω , respectively. The voltage supplied to the heaters was maintained constant to within 1 mV ($\pm 0.01\%$). The resistance of the heaters, measured after every test run, was found to remain constant to within $5 \text{ m}\Omega$ ($\pm 0.07\%$). The thermocouples were connected through a Fluke Helios I data acquisition system to an IBM PS/2 computer. Temperature readings were sampled at 0.1 Hz and averaged over a period of approximately 5 min. Heater power levels of 30 and 20 W were used as necessary to ensure that the element-to-coolant temperature difference was always greater than 7°C . The maximum temperature difference was 20°C , with a typical coolant temperature of 15°C .

Two static pressure taps of 0.06 cm diameter are located in the bottom wall to measure pressure drop across the array. The taps are connected to a Validyne pressure transducer. The transducer was calibrated against a U-tube manometer with a $\pm 0.3 \text{ N m}^{-2}$ (0.025 mm water) reading accuracy. The uncertainty in the pressure drop measurements was within $\pm 0.5 \text{ N m}^{-2}$.

The uniformity of flow in the water channel was verified before any tests were conducted, with a smooth wall in place of the heater array. Dye entrainment as well as hydrogen-bubble sheets were used to check the uniformity of the flow and to ensure that no major disturbances propagated from upstream into the test section.

Calculation of the heat transfer coefficient

Each element was assumed to be isothermal and the Plexiglas substrate was treated as being adiabatic

in the calculation of the heat transfer coefficient. Substrate conduction losses were estimated to constitute less than 0.4% of the total heater output. Conduction through the thermocouple and heater lead wires was estimated to be well below 0.6%. A simplified calculation, assuming an emissivity of 0.5 for partially-oxidized copper, yielded a radiation contribution to heat transfer of the order of 0.4% of the heater output. The emissivity value used is for air as the surrounding medium, since data are not available for emissivity in water.

Heat transfer coefficients were calculated for each individual heated element as follows:

$$h = (V^2/R)/[A(T_h - T_{ref})] \quad (1)$$

where V is the voltage applied, R the resistance of each heater, and T_h the element temperature. The active surface area of each element, A (16.77 cm^2), consists of the top surface and the sides. Two reference temperatures (T_{ref}) were used in the definition of h : the spanwise-averaged bulk-mean temperature of the fluid at the element location (T_m), and the adiabatic temperature of the element (T_{ad}). The effect of the choice of reference temperature will be examined in the next section. A detailed uncertainty analysis revealed uncertainties in the heat transfer coefficients obtained in this study to be within $\pm 4\%$.

Results are presented in terms of the non-dimensional parameters, Nusselt number and Reynolds number, defined as

$$Nu = hB/k; \quad Re = U_{ref}L_{ref}/\nu \quad (2)$$

where B is the element height, and ν the kinematic viscosity of the coolant fluid. Two definitions of Reynolds number were used. The first is the familiar channel Reynolds number, Re_H , where the reference velocity U_{ref} is the velocity at the entrance to the test section, and the characteristic dimension L_{ref} is the channel height, H . A second choice of Re is the array Reynolds number, Re_a , where L_{ref} is the element height B and U_{ref} is the array velocity defined as

$$U_a = U_m(C_d/C_{d0})^{1/2} \quad (3)$$

where U_m is the mean-inlet velocity and C_d the drag coefficient defined as

$$C_d = (P_{s,u} - P_{s,d})/(1/2\rho U_m^2). \quad (4)$$

The numerator in equation (4) is the difference between the static pressures upstream and downstream of the array, and represents the form drag encountered by the flow passing through the array (neglecting skin friction). The fraction of the incoming flow that actually flows through the array is a function of the channel height. The drag coefficient at the lowest channel height, C_{d0} , corresponds to the situation where almost all of the incoming flow passes through the array. As the channel height increases, a greater fraction of the flow bypasses the array, and a decrease in the drag coefficient results, indicating a decrease in the array velocity as a fraction of the mean-inlet velocity according to equation (3).

The array Reynolds number is then given by

$$Re_a = U_a B / \nu \quad (5)$$

The motivation for using the array Reynolds number is brought out in the next section. Moffat *et al.* [5] were the first to use this concept of array velocity. However, a different definition was used in their study and was based on a ratio of pressure coefficients, defined in terms of the difference between the total pressure upstream and the static pressure downstream of the array. The distinction in the definition of array velocity used in the present study from that used by Moffat *et al.* is to be noted.

Test matrix

Temperature and pressure drop measurements were obtained as a function of flow rate at four different channel heights (channel-to-element-height ratio, $H/B = 1.2, 1.9, 2.7, 3.6$). The flow rate was varied from 0.06 to 1.9 kg s⁻¹ in approximately 15 increments. The following spanwise (SS) and streamwise (or longitudinal, LS) spacings between elements of the array were investigated:

$$LS/B = 6.5, 4.3, 2.2, 1.1, 0.5$$

$$\text{(with constant } SS/B = 2.2)$$

$$SS/B = 6.5, 2.2, 0.5 \quad \text{(with constant } LS/B = 2.2).$$

The array with $LS/B = SS/B = 2.2$ was designated as the baseline configuration for which all 30 elements were heated. Use of an array with all elements heated allowed a comparison of the bulk-mean temperature (T_m) and the adiabatic element temperature (T_{ad}). Further, a fully heated array made it possible to investigate the behavior of heat transfer coefficients with increasing row number and to verify the spanwise uniformity of heat transfer coefficients of the elements in each row. Experiments to study the influence of spacing between elements were performed with only one heated element, the remaining elements being made of Plexiglas. The heated element was positioned in the fully developed region of the flow, which will be identified in the next section. Results were also obtained for a staggered array, where alternate rows in the baseline configuration were shifted sideways by one element width (i.e. by $SS/B = 2.2$), leading to an LS/B of 6.5.

Temperatures were also measured at each channel height with zero flow for the baseline configuration to determine natural convection heat transfer coefficients. After an initial rapid rise, the element temperature approached an asymptotic value when the rate of heat input to the element was equal to the rate of heat loss from the fluid within the array into the fluid away from the array. Natural convection coefficients were based on the average of the asymptotic temperatures reached by the interior elements of the array. The coefficients obtained in this manner agreed well with the values obtained by extrapolating the forced convection curves (Nu vs Re_H) to zero flow rate ($Re_H = 0$).

RESULTS AND DISCUSSION

The presentation of results will begin with the heat transfer and pressure drop results for the baseline configuration. The effects of changing the streamwise and spanwise spacing of elements are examined next. Correlations are proposed for data from all the spacings at the different channel heights, and for the staggered array. Finally, results from the present study are compared to studies in the literature.

Results for the baseline configuration

Heat transfer coefficients for the baseline configuration with $LS/B = SS/B = 2.2$ are presented in this section. All 30 elements were heated in these experiments.

Variations across rows and columns: fully developed region. The variation of heat transfer coefficient with row number is shown in Fig. 3 for two channel Reynolds numbers each at three channel heights. At $Re_H = 5150$, there is a drop in the heat transfer coefficient as the row number increases, reaching an asymptotic value by the fourth row. The dependence of the heat transfer coefficient on row number decreases both with increasing channel height and with decreasing Reynolds number. From an examination of the data in Fig. 3 and all other data from this study, it was deduced that the heat transfer coefficient can be considered to have reached a row-number-independent, fully developed value by the fourth row for all test runs. The attainment of fully developed conditions downstream of three to four rows was also observed by Moffat *et al.* [5] and Sparrow *et al.* [6].

Each data point in Fig. 3 represents the average of heat transfer coefficients across the five columns in each row. The maximum variation within each row was 5% for the lowest channel height, decreasing to 3% at the highest channel height. The flanking columns in each row had higher heat transfer coefficients than the interior columns, due to greater ventilation. In the interior three columns, the variation in heat transfer coefficient was well under 1% for all cases.

Based on this occurrence of row-independent heat transfer coefficients after the first three rows, a fully developed heat transfer coefficient was calculated for

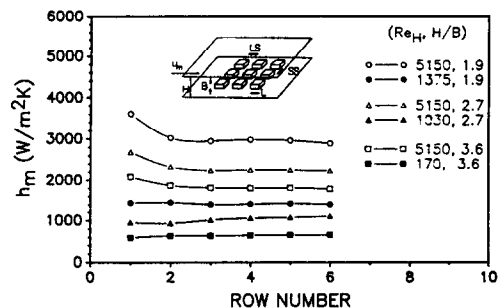


FIG. 3. Variation of heat transfer coefficient with row number.

the array at each flow rate. This was obtained as the average of heat transfer coefficients over the 15 elements in the last three rows of the array. In the rest of this paper, only fully developed heat transfer coefficients will be presented for each case.

Effect of channel height. The variation of the fully developed Nusselt number with channel height for five channel Reynolds numbers is shown in Fig. 4. The Nusselt number decreases with increasing H/B and with decreasing Re_H . As the channel height increases at a constant Re_H , the inlet velocity U_m decreases (equation (2)). In addition, the flow follows a path of least resistance, and more of the flow bypasses the array. This causes a lower local velocity in the array and results in the lower heat transfer coefficients seen in the figure. As channel height increases, the Nusselt number becomes less dependent on channel height and seems to approach an asymptotic value. This might indicate that beyond a certain H/B , there is only an insignificant change in the velocity seen by the array with further increases in the channel height, leading to an almost-invariant value for the heat transfer coefficient. It appears that at large values of H/B , the effect of the protruding elements is confined to a 'boundary layer' at the lower wall.

The decrease in the dependence of Nusselt number on channel height is seen from Fig. 4 to be less pronounced at the lower Reynolds numbers. The resistance offered by the array can be characterized by the pressure drop across the array. Since the pressure drop varies as the square of velocity, the resistance to flow decreases more rapidly than the Reynolds number. This implies that at lower Re_H , the array offers a smaller resistance to flow, less of the flow bypasses the array, and the channel height has a smaller influence on the heat transfer coefficient.

Adiabatic temperature. Adiabatic temperature is the temperature attained by an element when its own power is turned off while the rest of the array is powered. It thus represents the temperature of the heated wakes produced by the upstream elements. Heat transfer coefficients based on bulk-mean liquid temperature (h_m) were compared with those based on the element adiabatic temperature (h_{ad}). The coefficients differed in magnitude by an average of 5% at $H/B = 1.9$ and 3% at $H/B = 3.6$, T_{ad} being greater

than T_m . These results indicate that for the present study, either reference temperature (T_{ad} or T_m) can be used interchangeably in the heat transfer coefficient calculation, with a resulting uncertainty of less than 5%. A discussion of the choice of reference temperature is available in Moffat *et al.* [5].

Effect of Reynolds number. The Nusselt number is shown in Fig. 5 as a function of channel Reynolds number for the four different channel heights. In an attempt to separate the effect of buoyancy from the convective heat transfer coefficient, the superposition approach suggested by Acrivos [16] was used. In this approach, it is assumed that the Nusselt numbers due to natural convection and pure forced convection can be summed to yield an effective Nusselt number as follows:

$$Nu^n = Nu_F^n + Nu_N^n \quad (6)$$

The usual choice for the exponent, n , in the literature appears to be 3. The natural convection Nusselt number was calculated from the measured heat transfer coefficients at zero flow, and the forced convection Nusselt number was deduced from equation (6) using the measured values of Nu at various flow rates. Only the estimated purely forced convective component of heat transfer coefficient (Nu_F) is shown in Fig. 5. The difference between Nu and Nu_F was found to decrease as the Reynolds number increased and as the channel height decreased. This is expected, since the flow velocity increases in either instance and hence, less buoyancy effects occur. The total Nusselt number, Nu , was greater than Nu_F by less than 1% for most flow rates at $H/B = 1.2$, increasing to a maximum of 5% for $H/B = 3.6$ in the turbulent flow regime. In the data to be presented henceforth, only the total Nusselt number (Nu) is used in view of this small contribution of buoyancy in the turbulent flow regime for all channel heights.

The Nusselt number in Fig. 5 increases as channel height decreases, as seen previously in Fig. 4. Two distinct regimes can be identified in Fig. 5, indicating a transition from laminar to turbulent flow. Transition occurs at channel Reynolds numbers of approximately 700 for $H/B = 1.2$, 950 for $H/B = 1.9$, 1550 for $H/B = 2.7$, and 1900 for $H/B = 3.6$. These results

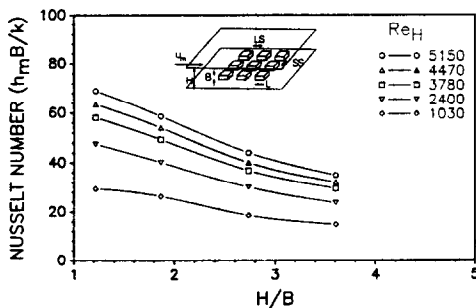


FIG. 4. Variation of Nusselt number with channel height.

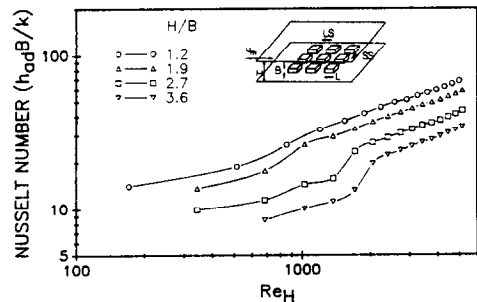


FIG. 5. Variation of Nusselt number with channel Reynolds number, baseline configuration.

correspond well with transition Reynolds numbers inferred from flow visualization.

Pressure drop. Results for the static pressure drop are presented in Fig. 6 in non-dimensional form as the drag coefficient defined in equation (4). At Reynolds numbers lower than 700 and 2000 respectively for the larger channel heights with $H/B = 2.7$ and 3.6 , the pressure drop decreases to become comparable in magnitude to the error in measurement. The data in these regions are not shown. At each channel height, the drag coefficient initially drops rapidly as the Reynolds number increases but soon reaches a steady value. The Reynolds numbers beyond which the drag coefficient becomes constant are approximately equal to those deduced previously for transition. This indicates that the drag coefficient decreases in the laminar regime as Reynolds number increases but attains a constant value in the turbulent regime. The results also show that as the channel height increases, pressure drop decreases sharply. In a typical case at a Reynolds number of 4800, the values of C_d were 0.55, 0.29, 0.17, and 0.10 for $H/B = 1.2, 1.9, 2.7,$ and 3.6 respectively. These drag coefficients correspond to actual pressure drops of 32, 7, 2, and 0.7 N m^{-2} .

Array Reynolds number. It is clear from Fig. 5 that Nusselt number is parametric in H/B . In an attempt to exclude H/B as an explicit parameter from the Nusselt number representation of Fig. 5, the array Reynolds number defined in equation (5) was used. The motivation for this definition is as follows. The channel height affects heat transfer by affecting the velocity to which the elements are exposed. The flow approaching the array partitions into a bypass flow over the array and a flow through the array, depending on the pressure drop in each of these flow paths. Since the skin friction due to the channel walls is small, most of the measured static pressure drop must be due to the form drag of the elements, which decreases with increasing channel height. To equalize pressure drops in the two flow paths, the bypass velocity would have to be much higher than the array velocity. The array velocity can be estimated from the mean-inlet velocity using pressure drop data, as given by equations (3) and (4). It is to be noted that, at the lowest channel height, $H/B = 1.2$, the average velocity

at any cross section of the array is nearly equal to the mean-inlet velocity since there is negligible bypass flow.

The variation of Nusselt number with array Reynolds number for the four channel heights is shown in Fig. 7. The adiabatic heat transfer coefficient is used to calculate Nusselt number for consistency with data to be presented shortly. Only data in the turbulent regime are presented since a correlation is not attempted in the laminar-transition regimes. Data for all but the lowest channel height are seen to collapse onto a straight line, showing that the array velocity is indeed the physically important reference velocity.

The fact that data for the lowest channel height lie on a separate line indicates that the mechanisms of heat transfer must in some way be different for this case. At the three larger channel heights, the top surface of each element is exposed to the bypass velocity. However, for the lowest channel height, there is little exposure for the top surface of elements to cooling flow, and hence very little convection occurs from the top. Since the top surface of an element constitutes about 40% of the total cooled surface area, the Nusselt numbers for the lowest channel height are lower.

Results for other array configurations

For this segment of the study, all but one of the 30 elements were made from Plexiglas. With only one element heated, the heat transfer coefficients that result from the data are based on the adiabatic element temperature, which is equal to the bulk-mean liquid temperature (T_m). The single heated copper element was placed in the central column of the fifth (penultimate) row of the array so as to locate it in the fully developed region of the flow. For the array with $LS/B = 6.5$, only four rows could be accommodated on the hatch, and the heated element was placed in the third row.

Streamwise and spanwise spacings. Streamwise spacing between elements was found to have a strong effect on the heat transfer coefficient. Figure 8 shows the heat transfer coefficient at five values of LS/B (with constant $SS/B = 2.2$) as a function of Re_H for $H/B = 3.6$. Results for all five spacings in Fig. 8 show

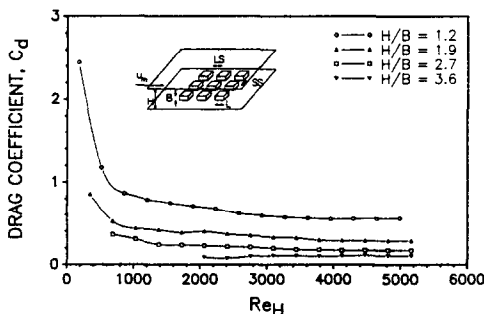


FIG. 6. Variation of pressure drop with channel Reynolds number, baseline configuration.

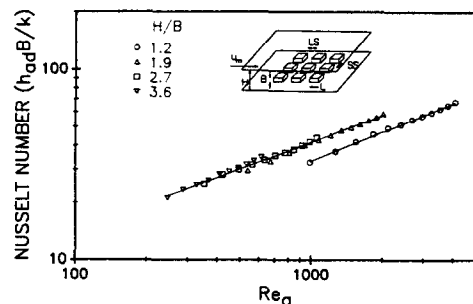


FIG. 7. Variation of Nusselt number with array Reynolds number, baseline configuration.

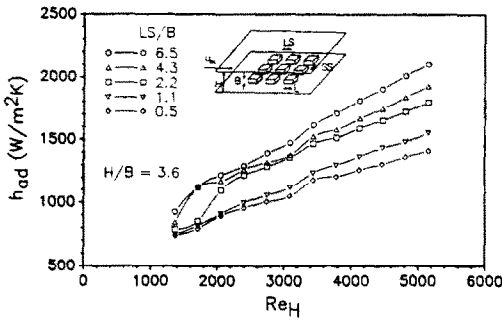


FIG. 8. Effect of streamwise spacing on adiabatic heat transfer coefficient, $H/B = 3.6$.

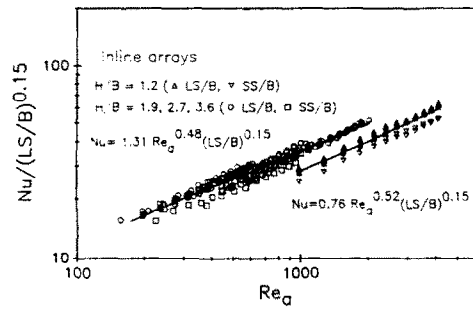


FIG. 9. Correlation of data for all inline spacings.

that the heat transfer coefficient increases with increasing streamwise spacing and with increasing Reynolds number. Data for the two smaller spacings, $LS/B = 0.5$ and 1.1 , lie in a distinct set towards the lower part of the graph, while data for the three larger spacings, $LS/B = 2.2, 4.3,$ and 6.5 , lie together in a higher group, implying two different flow regimes.

At smaller streamwise spacings, confined flow exists in the cavities between elements in each column. Heated fluid recirculates in these cavities and does not get carried away. In contrast, with the larger spacings between elements, it appears that the flow that separates from the leading edge of an element reattaches in the cavity just downstream. Heated fluid between elements is carried away by the main flow, resulting in higher heat transfer coefficients. Flow visualization, as well as an observation of the thermal wakes made visible due to their different refractive index, support this theory. The delineation of interacting and confined cavity flows demonstrated by the data corresponds to that suggested by Perry *et al.* [17] for two-dimensional ribs. In their study, it was proposed that the cavity flow is completely confined for an LS/B less than 2, with increasing interaction as LS/B increases beyond 2.

The effect of streamwise spacing on heat transfer coefficient at the lower channel heights with $H/B = 2.7$ and 1.9 (not shown) was similar to that observed above for $H/B = 3.6$. However, the results for $H/B = 1.2$ differed with regard to the value of LS/B at which the cavity flow changes from confined to interacting behavior. Cavity flow appeared to start interacting with the throughflow between columns (no bypass flow) at a streamwise spacing of $LS/B = 4.3$ in this case.

In a study using transverse ribs, Lehmann and Wirtz [8] found that the heat transfer coefficient increases with increasing streamwise spacing. Moffat and Ortega [14] observed that for transverse ribs, an upper limit occurred at an LS/B of 4 for the increase in heat transfer coefficient with increasing streamwise spacing. Such an upper limit might also exist for three-dimensional protruding elements, but no limit was encountered in the LS/B range of $0.5-6.5$ used in the present study.

Spanwise spacing was found to have a smaller effect

on the heat transfer coefficient compared to streamwise spacing. A variation in LS/B over the range $0.5-6.5$ causes a spread of 35–40% in the heat transfer coefficient at any channel height, whereas for the same range of variation of SS/B , the spread is only 15%. At the larger channel heights, data for the spacings of $SS/B = 2.2$ and 6.5 lie together, well above those for $SS/B = 0.5$ where the rows of elements behave like two-dimensional ribs with hot recirculation regions trapped between rows. At the lowest channel height of $H/B = 1.2$, however, the spacing of $SS/B = 2.2$ yields higher heat transfer coefficients than the other two spacings of $SS/B = 0.5$ and 6.5 . The heat transfer coefficient is lower when the spanwise spacing is either so small as to obstruct the flow (rows approach rib-like behavior) or large enough to allow little interaction of the wakes from neighboring elements. Heat transfer coefficients for all spanwise spacings are included in Fig. 9 to be discussed shortly.

Staggered array. Alternate rows of elements from the baseline configuration were staggered by one element width as shown in the inset of Fig. 10. The enhancement in heat transfer resulting from staggering the elements, when compared to the corresponding inline array, was of the order of 40% for $H/B = 1.2$, 18% for $H/B = 1.9$, 9% for $H/B = 2.7$, and 7% for $H/B = 3.6$. Staggering the elements yields the maximum advantage when most of the flow passes through the array, that is, at the lowest channel height. As the channel height is increased, the amount of bypass flow increases relative to the array flow, and staggering the elements has a diminishing impact on heat transfer. Results for the staggered array

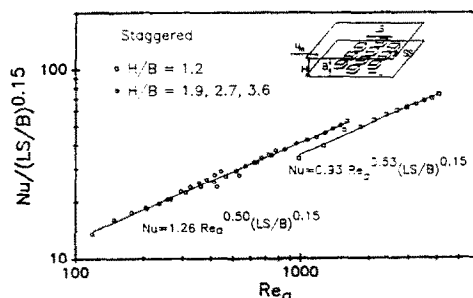


FIG. 10. Correlation of data for the staggered array.

are shown in Fig. 10 and discussed in a subsequent section.

Pressure drop. The pressure drop was observed to increase as the streamwise spacing was increased for all channel heights. The drag coefficient increased by approximately 150% at all channel heights for an increase in the streamwise spacing from an LS/B of 0.5 to 6.5.

The pressure drop for staggered arrays was greater than for the corresponding inline arrays, as expected. The difference in pressure drop between the two configurations was greatest at the lowest channel height and decreased as the channel height increased. At $H/B = 1.2$, pressure drop for the staggered array was greater than for the inline array by almost 110%, decreasing to a difference of 35% at $H/B = 1.9$, 20% at $H/B = 2.7$, and 18% at $H/B = 3.6$.

Overall heat transfer correlation

Heat transfer coefficients at the different channel heights for each array configuration discussed above were found to exhibit the same Reynolds number dependence when the array Reynolds number was used, just as was observed with the baseline array. An attempt was made to correlate the data for all the streamwise and spanwise spacings. The streamwise spacing, LS/B , was used as a parameter. Due to the limited influence of spanwise spacing on heat transfer coefficients, especially at the larger channel heights as discussed above, SS/B was not a parameter in the correlation. The resulting correlation, along with the experimental data for all the streamwise and spanwise spacings (274 points), is shown in Fig. 9. Data for the three larger channel heights at all spacings collect around a straight line in the log-log plane. A least-squares curve fit to this data yields the following correlating equation:

$$Nu = 1.31 Re_a^{0.48} (LS/B)^{0.15}. \quad (7)$$

Predictions using this equation differ from the experimental data by a standard deviation of 7%. Data for the lowest channel height collapse around a different line that lies below the line for the larger channel heights, as was seen in Fig. 7 for the baseline configuration. The correlating equation for the lowest channel height is given by

$$Nu = 0.76 Re_a^{0.52} (LS/B)^{0.15}. \quad (8)$$

The standard deviation of the experimental data for $H/B = 1.2$ from this equation is 6.5%.

The influence of spanwise spacing is evident in Fig. 9, especially at the lowest channel height. The two sets of data that lie below the rest of the data for $H/B = 1.2$ correspond to spanwise spacings with SS/B of 0.5 and 6.5. When only the streamwise spacings are considered in the correlation, the scatter in the data is much lower. The constant in equation (8) is then 0.70 and the Reynolds number exponent is 0.54, with a standard deviation of only 2.5%. This demonstrates that when the bypass flow is negligible (at the lowest chan-

nel height), the heat transfer coefficient of an element is sensitive to the wakes from surrounding elements.

Heat transfer coefficients for the staggered array are presented in Fig. 10. The ordinate is calculated with a value of 6.5 for LS/B . A comparison of Figs. 9 and 10 shows that the enhancement is most significant at the lowest channel height, as described earlier. Correlating equations for the staggered array are given as follows. For the larger three channel heights, the Nusselt number is given by

$$Nu = 1.26 Re_a^{0.50} (LS/B)^{0.15} \quad (9)$$

and for $H/B = 1.2$, the equation is

$$Nu = 0.93 Re_a^{0.53} (LS/B)^{0.15}. \quad (10)$$

The experimental data exhibit a standard deviation of 3.3% from equation (9) for $H/B = 3.6$, 2.7, and 1.9, and 2.4% from equation (10) for $H/B = 1.2$.

Comparison with other studies

The liquid-cooling results of the present study are compared with several air-cooling studies in the literature. The correlations proposed above cannot be used directly in the comparisons since the array Reynolds number is not available for these studies. Though Moffat *et al.* [5] also used an array Reynolds number in correlating their data for air cooling, a different definition was used in their study. The comparisons made here are based on the channel Reynolds number. Experimental data used from the present study in the comparisons are those that approximate the geometry of the other studies as closely as possible, and are indicated on the figure.

The Nusselt numbers for the three-dimensional protruding elements from the present study are contrasted with those of Moffat *et al.* [5] and Sparrow *et al.* [6] in Fig. 11, to investigate scaling between air and water. For this purpose, the Nusselt numbers from each study are scaled with $Pr^{0.35}$. Prandtl number was not a parameter of investigation in any of these studies. Therefore, the exponent of 0.35 for the Prandtl number was chosen based on the suggestion of Kececy *et al.* [3]. Prandtl number scaling provides good agreement between the present study and that of Sparrow *et al.*, with only a 2.5% deviation at the higher Reynolds numbers.

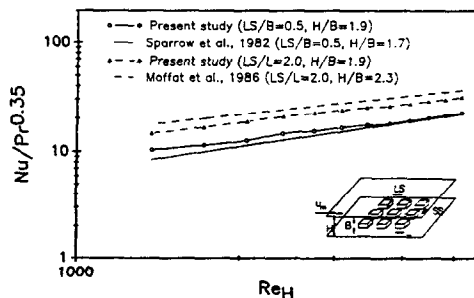


Fig. 11. Comparison of present study with air-cooling studies of Moffat *et al.* [5] and Sparrow *et al.* [6].

The results of Moffat *et al.* follow the same Reynolds number dependence as the present study since the slopes of the two curves are equal (0.65), but their results lie 18% higher than the present results. One possible explanation for this discrepancy is the difference in the chip length-to-height ratio (L/B) of the two studies ($L/B = 1$ for Moffat *et al.*, 2 for the present study). There is evidence in the literature that the aspect ratio of the heat source element affects the heat transfer coefficient. In a study with ribs, Wieghardt [18] showed that the drag coefficient increases as the rib length-to-height ratio (L/B) decreases, for values of this ratio less than 5. Most electronic chips fall into this category and it would be reasonable to expect the heat transfer coefficient to show an analogous trend. The higher heat transfer coefficients of Moffat *et al.* could thus be due to their 'taller' chips, with a smaller L/B ratio than that of the present study. From this discussion, the chip length-to-height ratio (L/B) suggests itself as a parameter for future investigation.

CONCLUDING REMARKS

The research reported here appears to be the first systematic investigation of single phase liquid cooling of arrays of large protruding elements. Heat transfer and pressure drop measurements were obtained at several channel heights and over a range of element spacings.

Transition was found to be strongly dependent on channel height. The channel Reynolds number for transition was 700 for an H/B of 1.2 increasing to 1900 for an H/B of 3.6. Fully developed conditions with respect to heat transfer were found to exist at the fourth and all subsequent rows of the array for all conditions of this study.

The Nusselt number decreased with increasing H/B and approached an asymptotic value for large H/B . In the turbulent forced convective regime, the contribution of free convection to the overall heat transfer coefficient was well within 5%.

All the data were successfully correlated using an array Reynolds number, which accounted for the partitioning of the approach flow into a bypass flow and an array flow. There is no bypass flow at the lowest channel height where the top wall is very close to the tops of elements, and this leads to lower heat transfer coefficients (at a given array Reynolds number) at this channel height. The element height B was found to be the appropriate characteristic dimension for non-dimensionalization.

Streamwise spacing between elements was found to have a more significant effect on heat transfer than the spanwise spacing. The heat transfer coefficient increases with increasing streamwise spacing, due to an increasing interaction between the cavity flow and the main flow. Staggering the elements of the array caused increases in the heat transfer coefficients by amounts ranging from 40% at the lowest channel height to 7% at the highest.

Results from the present study agree well with results from the literature for air cooling of elements of similar shape when both are normalized against Prandtl number. However, the agreement is less satisfactory when air-cooling results from 'taller' elements are considered. This suggests the length-to-height dimensional ratio of the element as a potentially important parameter for investigation.

Acknowledgements—This work was sponsored by an IBM Young Faculty Development Grant, and by the Thermal Systems and Engineering Division of the National Science Foundation (Grant # CBT-8807838). The support and excellent suggestions of R. C. Chu and R. E. Simons of IBM Corporation are gratefully acknowledged.

REFERENCES

1. F. P. Incropera (Editor), Research needs in electronic cooling, *Proc. NSF Workshop*, Purdue University (1986).
2. F. P. Incropera, J. Kerby, D. F. Moffat and S. Ramadhyani, Convection heat transfer from discrete sources in a rectangular channel, *Int. J. Heat Mass Transfer* **29**, 1051–1058 (1986).
3. F. J. Kelecy, S. Ramadhyani and F. P. Incropera, Effect of shrouded pin fins on forced convection cooling of discrete heat sources by direct liquid immersion, *Proc. ASME JSME Heat Transfer Conf.*, Hawaii, pp. 387–394 (1987).
4. K. R. Samant and T. W. Simon, Heat transfer from a small, high-heat-flux patch to a subcooled turbulent flow, *ASME AIAA Thermophysics Conf.*, Boston (1986).
5. R. J. Moffat, D. E. Arvizu and A. Ortega, Cooling electronic components: forced convection experiments with an air-cooled array, *ASME HTD*-Vol. 48, pp. 17–27 (1985).
6. E. M. Sparrow, J. E. Niethammer and A. Chaboki, Heat transfer and pressure drop characteristics of arrays of rectangular modules encountered in electronic equipment, *Int. J. Heat Mass Transfer* **25**, 961–973 (1982).
7. A. M. Anderson and R. J. Moffat, Direct air cooling of electronic components: reducing component temperatures by controlled thermal mixing, *ASME Winter Annual Meeting*, Chicago (1988).
8. G. L. Lehmann and R. A. Wirtz, The effects of variations in streamwise spacing and length on convection from surface mounted rectangular components, *ASME HTD*-Vol. 48, pp. 39–47 (1985).
9. J. C. Han, L. R. Glicksman and W. M. Rohsenow, An investigation of heat transfer and friction characteristics for rib-roughened surfaces, *Int. J. Heat Mass Transfer* **21**, 1143–1156 (1978).
10. B. A. Kader and A. M. Yaglom, Turbulent heat and mass transfer from a wall with parallel roughness ridges, *Int. J. Heat Mass Transfer* **20**, 345–357 (1977).
11. J. R. Garratt and B. B. Hicks, Momentum, heat, and water vapor transfer to and from natural and artificial surfaces, *Q. J. R. Met. Soc.* **99**, 680–687 (1973).
12. R. L. Webb, E. R. G. Eckert and R. J. Goldstein, Heat transfer and friction in tubes with repeated-rib roughness, *Int. J. Heat Mass Transfer* **14**, 601–617 (1971).
13. W. Nakayama, Thermal management of electronic equipment: a review of technology and research topics, *Appl. Mech. Rev.* **39**, 1847–1868 (1986).
14. R. J. Moffat and A. Ortega, Direct air-cooling of electronic components. In *Advances in Thermal Modeling of Electronic Components and Systems* (Edited by A. Bar-Cohen and A. D. Kraus), Vol. 1, Chap. 3, Hemisphere, New York (1989).

15. A. E. Bergles. Liquid cooling for electronic equipment, Int. Symp. on Cooling Technol. for Electronic Equipment, Hawaii (1987).
16. A. Acrivos. On the combined effect of forced and free convection heat transfer in laminar boundary layer flows, *Chem. Engrg Sci.* 21, 343-349 (1966).
17. A. E. Perry, W. H. Schofield and P. H. Joubert. Rough wall turbulent boundary layers, *J. Fluid Mech.* 37, 193-211 (1969).
18. K. Wieghardt, see H. Schlichting, *Boundary Layer Theory*, 7th Edn, p. 655. McGraw-Hill, New York (1979).

CARACTERISTIQUES DE TRANSFERT THERMIQUE POUR UN ARRANGEMENT D'ELEMENTS PROTUBERANTS EN CONVECTION FORCEE MONOPHASIQUE

Résumé—Des expériences sont conduites pour déterminer les coefficients de transfert convectif de chaleur pour des arrangements en ligne ou en quinconce de 30 éléments protubérants disposés en six rangées. Le nombre de Reynolds basé sur la hauteur de canal varie de 150 à 5150. La hauteur du canal varie selon les valeurs 1,2, 1,9, 2,7 et 3,6 hauteurs d'élément. Les espacements longitudinaux et transversaux entre les éléments varient jusqu'à un maximum de cinq valeurs entre 0,5 et 6,5 fois la hauteur de l'élément, pour chaque hauteur du canal. Les pertes de pression sont mesurées dans chaque cas. Les nombres de Reynolds de transition sont déduits des données de transfert thermique. Les données pour tous les espacements sont unifiées en utilisant un nombre de Reynolds d'arrangement qui tient compte de la partition de l'écoulement en écoulements de bypass et de nappe. On étudie l'intervention du nombre de Prandtl en considérant les résultats avec l'air et l'eau.

WÄRMEÜBERGANG AN EINER RIPPENANORDNUNG IN EINPHASIGER ERZWUNGENER STRÖMUNG

Zusammenfassung—Der konvektive Wärmeübergang an wassergekühlten, fluchtenden und versetzten Rippenanordnungen (30 Elemente in 6 Reihen) wird untersucht. Die mit der Kanalhöhe gebildete Reynolds-Zahl liegt zwischen 150 und 5150. Die Höhe des Strömungskanals wird auf das 1,2-, 1,9-, 2,7- und 3,6-fache der Rippenhöhe eingestellt. Die Rippenabstände in und quer zur Strömungsrichtung werden für jede Kanalhöhe auf höchstens 5 Werte eingestellt, die zwischen dem 0,5- und 6,5-fachen der Rippenhöhe liegen. Für alle Fälle wird der Druckverlust bestimmt. Die Übergangs-Reynolds-Zahl wird aus den Ergebnissen für den Wärmeübergang ermittelt. Die Ergebnisse für alle untersuchten Rippenabstände werden mit einer Anordnungs-Reynolds-Zahl korreliert, die eine Aufspaltung der Strömung in Haupt- und Nebenstrom berücksichtigt. Zusätzlich wird der Einfluß der Prandtl-Zahl durch Versuche mit Luft und Wasser untersucht.

ХАРАКТЕРИСТИКИ ТЕПЛОПЕРЕНОСА ОТ НАБОРА ВЫСТУПАЮЩИХ ЭЛЕМЕНТОВ ПРИ ОДНОФАЗНОЙ ВЫНУЖДЕННОЙ КОНВЕКЦИИ

Аннотация—Проводятся эксперименты для определения коэффициентов конвективного теплопереноса при водном охлаждении 30 нагретых выступающих элементов, расположенных в шесть рядов в коридорном и шахматном порядке. Значение числа Рейнольдса, рассчитываемое по высоте канала, изменяется от 150 до 5150. Высота канала варьируется в диапазоне 1,2; 1,9; 2,7 и 3,6 значений высоты элементов. Промежутки между элементами в направлении течения и по размаху изменяются в диапазоне пяти значений при варьировании высоты элементов от 0,5 до 6,5 в зависимости от высоты канала. Во всех случаях изменяются перепады давления. По полученным данным для теплопереноса установлены переходные значения числа Рейнольдса. Приведено соотношение между измеренными данными для всех диапазонов с использованием числа Рейнольдса для решетки, учитывающее разделение течения на область обтекания и течение в решетке. Исследуется масштабирование результатов по числу Прандтля для воздуха и воды.